Experimental Survey of the Strain Energy Density Function of Isoprene Rubber Vulcanizate

S. Kawabata,* M. Matsuda, K. Tei, and H. Kawai

Department of Polymer Chemistry, Kyoto University, Kyoto 606, Japan.
Received December 10, 1979

ABSTRACT: An experimental survey of the strain energy density function of an isoprene rubber vulcanizate is carried out by biaxial extension of a sheet specimen. The first derivatives of the strain energy density function with respect to I_1 and I_2 are obtained from the biaxial stress–strain measurement, where I_1 and I_2 are the first and the second invariants of Green's deformation tensor, respectively. The measurement of these derivatives is done over a wide range of biaxial deformation, $3.005 < I_1 < 20$ and $3.005 < I_2 < 90$, in the temperature range 273–353 K. Special care has been taken with the stress and strain measurements in the relatively small deformation region in order to prevent error in the derived values of the derivatives of the strain energy density function. From the result, it is concluded that the strain energy density function should be given by the sum of the two separate terms: $W = CT(I_1 - 3) + \beta(I_1,I_2)$. It has been found that both $\partial\beta/\partial I_1$ and $\partial\beta/\partial I_2$ are more sensitive to changes in I_2 than in I_1 and the value of $\beta(I_1,I_2)$ accounts for, in the case of $I_1 = I_2 = 10$, for example, 32.5% of the whole strain energy density W.

Introduction

In the 1930s and 1940s the kinetic theory of a molecular chain was developed[1-7] to interpret the elastic behavior of rubber vulcanizates. From the theory two important conclusions have been derived with respect to the form of the strain energy density function for an ideal rubber. First, the strain energy density, which will be denoted by W in this paper, depends on the deformation in such a manner that W is proportional to $I_1 - 3$, where I_1 is the first invariant of Green's deformation tensor. Second, W is proportional to absolute temperature. Many researchers began to examine this simple functional form of the W function. In the case of incompressible bodies such as rubber vulcanizates, biaxial deformation testing is necessary for the experimental determination of the general W function.[8-13]

The first biaxial extension experiment was carried out by Treloar in 1943[6] for a natural-rubber vulcanizate. After Treloar's experiment, Rivlin and Saunders[14] experimentally examined the room-temperature functional form of W in its two derivative forms in terms of I_1 and I_2, respectively, by a method similar to Treloar's and explained that W was a function not only of I_1 but also of I_2, where I_2 is the second invariant of Green's deformation tensor. Several biaxial experimental works[15-18] were carried out immediately after Rivlin and Saunders' experiments and confirmed that $\partial W/\partial I_2$ was not zero. These experimental results have attracted the attention of many researchers, and experimental studies have been carried out to obtain additional details about the W function; however, most of these studies have been carried out by means of Mooney–Rivlin plots from uniaxial data based on Mooney's equation[20] for the W function. As already pointed out,[27] this method is not always appropriate for a survey of the form of the W function.

The biaxial experiments were revived by Blatz and Ko[21] in 1962 and then by Zapas et al.,[19] Landel et al.,[22] Becker,[23] Kawabata et al.,[24] and Treloar et al.[25] Kawabata and co-workers examined the functional form of the partial derivatives of the strain energy density function, $\partial W/\partial I_1$ and $\partial W/\partial I_2$, for several rubber vulcanizates by using a new biaxial tensile instrument.[24] They pointed out that these derivatives do not take on constant values but change their values with both I_1 and I_2 over a wide deformation range and that these changes are especially evident in the relatively small deformation region.[26,27] The temperature dependence of these derivative functions was also examined by these biaxial experiments for the first time[28] and it was shown that $\partial W/\partial I_1$ is nearly proportional to absolute temperature but that $\partial W/\partial I_2$ is almost independent of the temperature. In 1973, Kawabata experimentally demonstrated that $\partial W/\partial I_2$ could take on negative values in the small-deformation region and became interested in the relation between this behavior and the intermolecular forces.[26]

However, it was also pointed out at the same time that considerable errors in both $\partial W/\partial I_1$ and $\partial W/\partial I_2$ will arise from a small error in the measurements of the stress and the strain in the biaxial deformation experiment in the relatively small deformation region. Thus a highly accurate experiment is necessary for obtaining reliable information about the functional forms of $\partial W/\partial I_1$ and $\partial W/\partial I_2$ in this region. "Relatively small deformation" means deformation such that each of the values of I_1 and I_2 is less than about 4.

In 1974, precise equipment for biaxial extension measurements in the small-deformation region was designed by Kawabata[29] to connect the data obtained from this new equipment with the data obtained from the first equipment. The latter is sufficiently accurate for measurements in the relatively large deformation region, that is, the region $I_1 > 4$ and $I_2 > 4$. In this paper, a complete set of data which covers the relatively small and the large deformation regions is presented for an isoprene rubber vulcanizate, using these two biaxial extension devices at several temperatures.

Theory

Consider a homogeneous biaxial deformation of an elastic and continuous body. In a rectangular coordinate system X_i ($i = 1, 2, 3$) taken along the principal axes of strain, the principal stresses σ_i ($i = 1, 2, 3$) for an incompressible body are expressed as functions of the principal stretch ratios λ_i ($i = 1, 2, 3$) as follows:[9]

$$\sigma_1 = \frac{2}{\lambda_1}\left(\lambda_1^2 - \frac{1}{\lambda_1^2\lambda_2^2}\right)\left(\frac{\partial W}{\partial I_1} + \lambda_2^2\frac{\partial W}{\partial I_2}\right) \quad (1)$$

$$\sigma_2 = \frac{2}{\lambda_2}\left(\lambda_2^2 - \frac{1}{\lambda_1^2\lambda_2^2}\right)\left(\frac{\partial W}{\partial I_1} + \lambda_1^2\frac{\partial W}{\partial I_2}\right) \quad (2)$$

where the relation $\lambda_3 = (\lambda_1\lambda_2)^{-1}$ has been used. The notation is as follows: W, strain energy density function as a function of I_1 and I_2; σ_1 and σ_2, principal stresses along the X_1 and X_2 axes (the stress is expressed here as the engineering stress, which is defined by the force per unit area in the undeformed state); λ_1, λ_2, and λ_3, principal stretch ratios along the X_1, X_2, and X_3 directions; I_1, I_2,

0024-9297/81/2214-0154$01.00/0

and I_3, invariants of Green's deformation tensor, given by the principal stretch ratios.[26,27] From eq 1 and 2, the following equations are obtained:

$$\frac{\partial W}{\partial I_1} = \frac{1}{2(\lambda_1^2 - \lambda_2^2)}\left[\frac{\lambda_1^3\sigma_1}{\lambda_1^2 - \lambda_1^{-2}\lambda_2^{-2}} - \frac{\lambda_2^3\sigma_2}{\lambda_2^2 - \lambda_1^{-2}\lambda_2^{-2}}\right] \quad (3)$$

$$\frac{\partial W}{\partial I_2} = \frac{1}{2(\lambda_2^2 - \lambda_1^2)}\left[\frac{\lambda_1\sigma_1}{\lambda_1^2 - \lambda_1^{-2}\lambda_2^{-2}} - \frac{\lambda_2\sigma_2}{\lambda_2^2 - \lambda_1^{-2}\lambda_2^{-2}}\right] \quad (4)$$

$\partial W/\partial I_i$ (i = 1, 2) can be determined by the set of σ_1 and σ_2 corresponding to the set of λ_1 and λ_2, and those stresses and stretch ratios are measured by the biaxial extension experiment. In general, each $\partial W/\partial I_i$ is a function of both I_1 and I_2 and can be obtained only by a biaxial deformation experiment for various sets of λ_1 and λ_2 which may be converted into I_1 and I_2.

Experimental Method

Biaxial Extension Experiment. Two types of biaxial extension equipment have been utilized. One of them, which we will call "the first instrument", was built in 1966. A specimen consisting of a square sheet 11.5 cm on a side and 1 mm in thickness is clamped at its edge by nine chucks for each of its four sides and then simultaneously stretched biaxially in two orthogonal directions. Two servo-controlled systems are mounted on the equipment, independent of each other, for stretching along each of these two directions. The chucks clamping each of the four sides of the specimen are mounted on a rail bar with ball bearings so that each chuck is able to move freely on the rail during the motion of the rail bar for stretching. The tensile forces along the two directions are detected separately by two independent systems of force measurement. The forces which are elongating the specimen are transmitted through each of the chucks to the rail bar and then to the force-measuring system. The stretch ratio of the specimen along each direction is measured by a potentiometer which detects the movement of the rail bar. However, direct measurement of the distance between two markings put on the specimen was made for precise measurements in the case of biaxial stress relaxation experiments, which are the main experiments reported here. Details of this equipment have been presented in our previous papers.[24,26] In this equipment, the maximum tensile force being applied for each direction is 1000 N, and the maximum stretch ratio is 6 in the case of the 11.5 cm × 11.5 cm square sample.

A problem arose with this equipment in the measurements for the relatively small deformation region. It was found that a frictional component distorted the measured force. Each chuck is supported on the base of the machine with a supporting roller, and the frictional component originates at the contact point between the surface of the supporting roller and the base. This small error in the force measurement results in a magnified error in each of the values of $\partial W/\partial I_1$ and $\partial W/\partial I_2$, especially in the small-deformation region.

For the purpose of eliminating this frictional effect, the second equipment for biaxial extension testing was built in 1974,[29] and some improvements for precise measurement in the small-deformation region were made in this equipment. A schematic diagram is shown in Figure 1. As shown in the figure, each of the chucks is mounted on the chuck rail with no other support. In addition, one more improvement in the mechanism was made as follows. The chuck rails facing each other move in opposite directions at the same time with the same velocity. Therefore, the center position of the specimen remains unchanged during the stretching of the specimen. This mechanism enables us to use a traveling microscope to measure the amount of the stretch with a high degree of accuracy.

The scatter in the measured values of $\partial W/\partial I_1$ and $\partial W/\partial I_2$ for this region has been remarkably reduced by the use of this improved equipment. Therefore, the first apparatus has been used for the large-deformation experiments. In addition, it has been confirmed that the data obtained from these two pieces of equipment are in good agreement with each other in the overlap region of the experiments. We consider the agreement between the data from these completely separate experiments proof of the reliability of the data. Each apparatus is covered completely by a box and the temperature inside the box is controlled over the range 273–353 K.

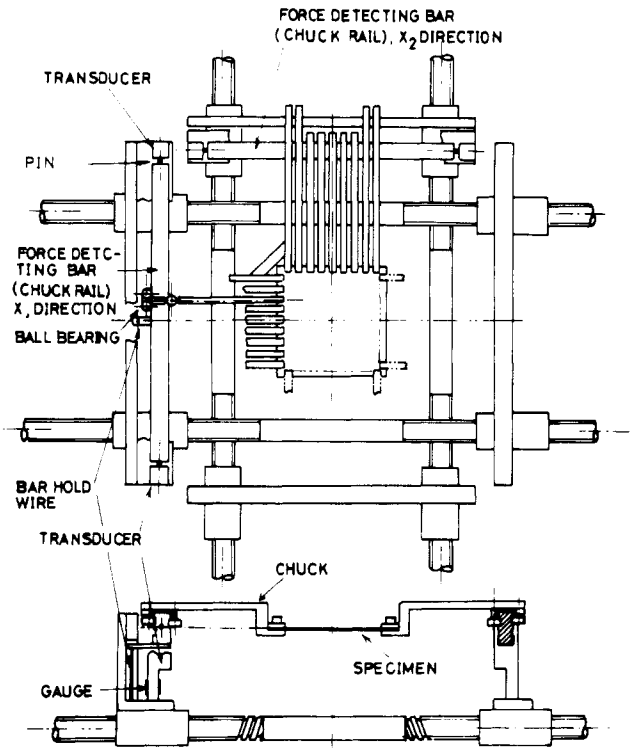

Figure 1. Biaxial extension equipment which has been improved for the precise measurement in the relatively small deformation region.

Table I
Composition and Conditions of Vulcanization[a]

	phr[b]		phr[b]
IR-2200	100	MBTS	1
ZnO	5	TMTD	0.1
St acid	1	S	2
SP	1		

[a] Cure: 418 K, 30 min. [b] Parts per hundred parts of rubber by weight.

Sample and Its Preliminary Examination. A vulcanized isoprene rubber (IR) was used in these measurements. The composition and the conditions of vulcanization are shown in Table I. The crystallization behavior of this sample was examined by a volume-dilatation measurement over the temperature range 253–283 K, which is taken to be equivalent to the lower temperature range in which the biaxial extension experiment was carried out. However, no indication of crystallization behavior has been observed in these experiments, even after several hours. This time interval is equivalent to the longest exposure period in the biaxial extension experiments.

A volume-compression experiment was also carried out in order to determine the compressibility of this vulcanizate. A cylindrical specimen was compressed along its axis direction and the strain along the radial direction was kept zero during the compression. The stress–strain relation is shown in Figure 2. The slope in this relation is given by the infinitesimal elasticity theory as

$$\frac{\sigma_3}{\epsilon_3} = \frac{1-\nu}{(1+\nu)(1-2\nu)}E \quad (5)$$

where σ_3 and ϵ_3 are the compressional stress and strain, respectively, and ν is Poisson's ratio. The Young's modulus E was measured from uniaxial extension experiments. Poisson's ratio obtained for this rubber vulcanizate is between 0.499 914 and 0.499 918 at room temperature.

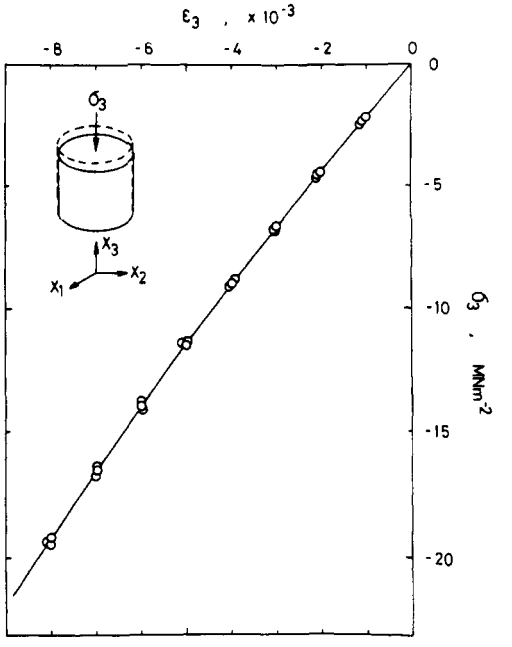

Figure 2. Stress–strain relation for a volume-compression test.

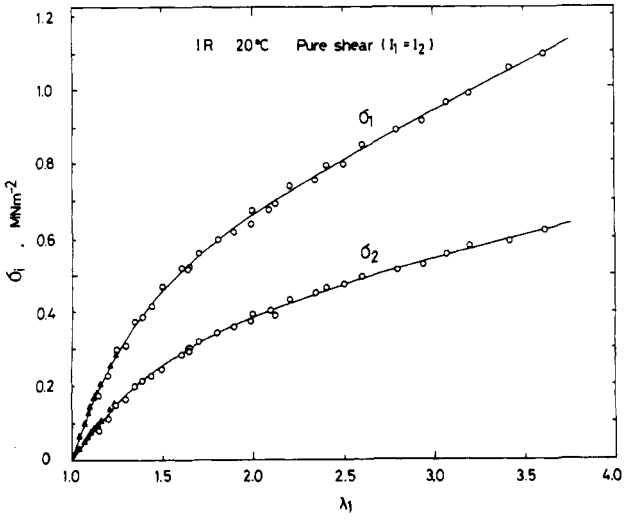

Figure 3. Isochronal (5 min) data of the stress and stretch ratio relations in pure shear at 20 °C: (○) original tester; (▲) modified tester.

From this result, it is concluded that the sample can be considered to be incompressible for the purpose of the calculation of $\partial W/\partial I_i$ from the stress and the stretch ratios in the biaxial experiments, using eq 3 and 4.

Experimental Procedure and Data Processing. The stress relaxation during the 20 min after the application of strain is about 1% of the initial stress which was measured a few seconds after the deformation. Although the time dependence in the stress–strain relation of this vulcanizate is not remarkable, the stress relaxation experiment was carried out and the isochronal values at 5 min were measured in order to eliminate the time effect completely. The stresses and the strains of the specimen were measured 5 min after the specimen was deformed; then the deformation was removed and the specimen was placed aside for a 5-min rest until the next deformation was applied. In the case of the relatively large deformation experiments, several specimens of the same vulcanizate were prepared and used alternately in order to give them sufficient time to recover from the deformation history of the specimen.

A small amount of scattering in the data still remains, as shown in Figure 3. In this figure, as an example, the isochronal stress and the stretch ratio relation under a pure-shear deformation (or strip biaxial extension) is shown by plotting the stress relaxation

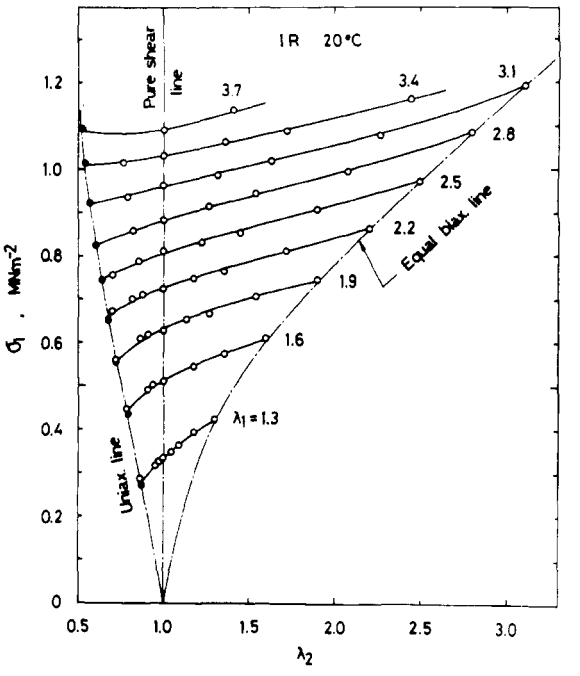

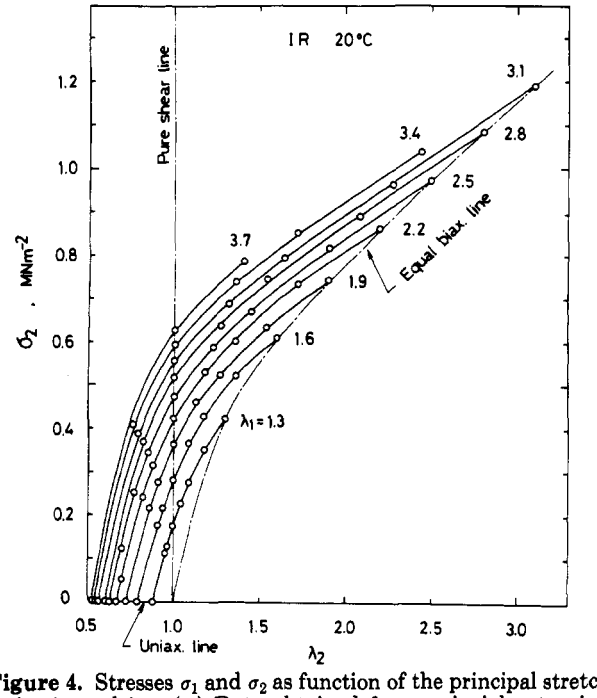

Figure 4. Stresses σ_1 and σ_2 as function of the principal stretch ratios λ_1 and λ_2. (●) Data obtained from uniaxial extension experiments using a ring specimen.

data at 5 min, and the most-probable relation for each σ_i is estimated by least-squares and shown as a solid line. The stress–stretch ratio relations for many other different deformations were examined by plotting them on several lines of constant $(\lambda_2 - 1)/(\lambda_1 - 1)$ in the same manner as shown in Figure 3 to eliminate the scattering of the raw data. From such stress–stretch ratio relations, an overall representation of these relations was made in Figure 4. Finally, the values of $\partial W/\partial I_i$ at constant I_1 or I_2 were calculated based on the data shown in Figure 4, using an extrapolation method. These procedures are important for obtaining reliable values of $\partial W/\partial I_i$ because a small amount of error in the raw data of the stress and stretch ratio relations causes magnified errors in the calculated values of $\partial W/\partial I_i$.

The triangle symbols in Figure 3 indicate the data obtained from the improved equipment built for a measurement in the small-deformation region. The scattering in the data obtained from this equipment is small enough to obtain reliable values of $\partial W/\partial I_i$ in the small-deformation region. Moreover, curves of the

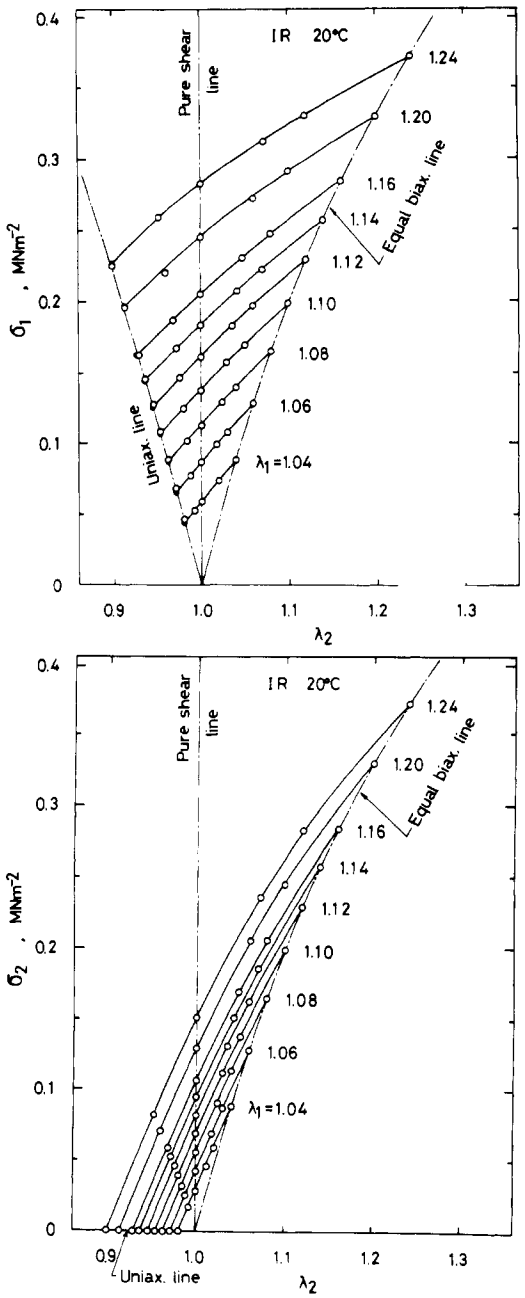

Figure 5. Stress and stretch ratio relations in the small-deformation region of Figure 4.

data from these two completely separate equipments are smoothly connected with each other. This is also proof of the reliability of the data obtained from these two pieces of equipment, as mentioned earlier.

Results

Results of the Experiment at 293 K. The stresses σ_1 and σ_2 obtained in the large-deformation biaxial extension experiment at 293 K are shown in Figure 4. The data in the small-deformation region for σ_1 and σ_2 are shown in Figure 5, using magnified coordinate scales to show the details precisely. The numerical data are given in Table II, along with the values of $\partial W/\partial I_1$ and $\partial W/\partial I_2$ which are calculated from the stresses and stretch ratios by using eq 3 and 4, respectively.

The values of $\partial W/\partial I_1$ and $\partial W/\partial I_2$ are plotted in Figure 6 with I_2 and I_1 abscissas. The details of these functions in the relatively small deformation region are shown in Figure 7, where the scale of the abscissa is enlarged. It is

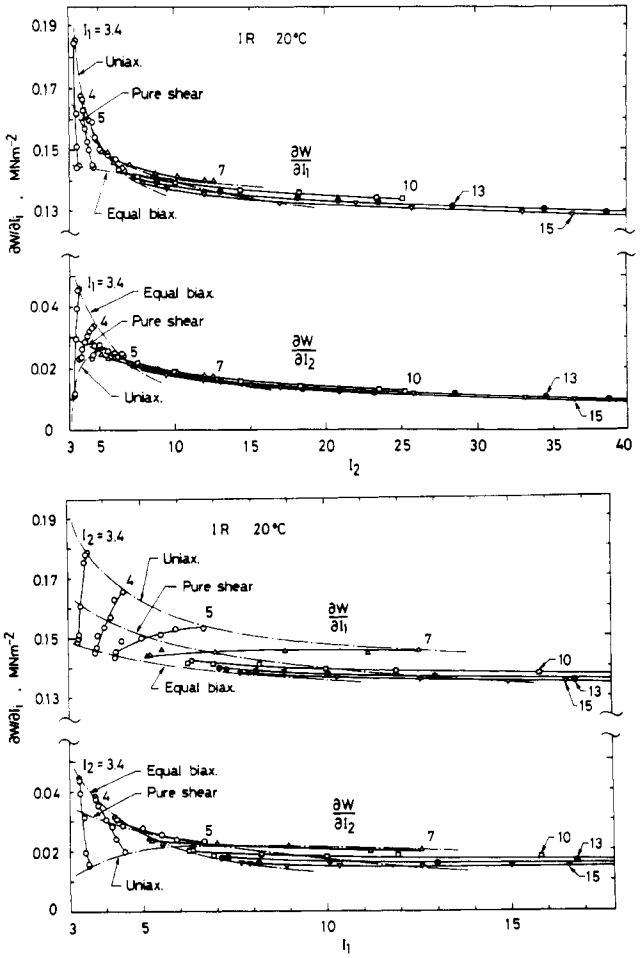

Figure 6. Plot of $\partial W/\partial I_1$ and $\partial W/\partial I_2$ against I_1 and I_2 at 20 °C.

clearly shown that the value of $\partial W/\partial I_2$ tends to go down and take a negative value at very small deformations. On the other hand, the value of $\partial W/\partial I_1$ goes up like a mirror reflection of the trend of $\partial W/\partial I_2$.

Temperature Dependence. With respect to the temperature dependence of $\partial W/\partial I_1$ and $\partial W/\partial I_2$, a series of biaxial extension experiments has been carried out over the temperature range 273–353 K. The results are shown in the top portion of Figure 8 and the detail in the small-deformation region is shown in the bottom portion of Figure 8, with I_2 as abscissa. The temperature dependence of $\partial W/\partial I_1$ is clearly observed in these figures. On the other hand, no dependence of $\partial W/\partial I_2$ on temperature is observed. These relations are shown in Figure 9 for the cases of $I_1 = 4$ and $I_2 = 3.88$, 4.00, 4.31, and 4.47, respectively. As seen in this figure, all of the slopes of the $\partial W/\partial I_1$ lines are almost equal to each other and a straight line may be drawn from a point at 0 K on the abscissa so as to be parallel to all these $\partial W/\partial I_1$ lines. It has been found that the temperature dependence of $\partial W/\partial I_1$ for the other deformations studied here is also parallel to this broken line. This is an important relation for the derivation of the functional form of the W function as shown below.

Discussion

It is clearly shown that the $\partial W/\partial I_1$ and the $\partial W/\partial I_2$ functions are not constant with respect to either I_1 or I_2 and that the functional forms of these relationships are complicated, especially in the relatively small deformation region.

Figure 10 shows $\partial W/\partial I_1$ and $\partial W/\partial I_2$ for pure-shear deformation to illustrate a typical trend of each of $\partial W/\partial I_i$

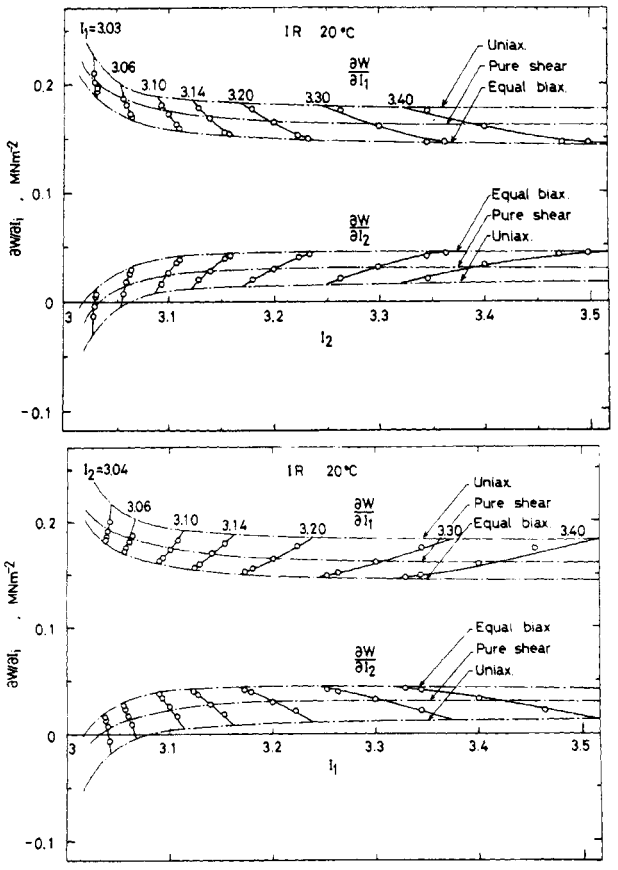

Figure 7. Plot of $\partial W/\partial I_1$ and $\partial W/\partial I_2$ in the small-deformation region.

functions over the whole range of I_2 (=I_1). As shown in the figure, the sum $\partial W/\partial I_1 + \partial W/\partial I_2$ in the very small deformation region assumes an almost constant value even though the values of both $\partial W/\partial I_i$ change dramatically in this region. As is well-known, the finite theory of elasticity deduces relation 6 for the incompressible body in its pure-shear deformation

$$E = \lim_{I_1,I_2 \to 3} 6\left(\frac{\partial W}{\partial I_1} + \frac{\partial W}{\partial I_2}\right) \tag{6}$$

where E is Young's modulus. $\partial W/\partial I_i$ on the right side of this equation should be obtainable by the pure-shear experiment. In our experiment, the value of E from uniaxial extension was 1.085 MN m^{-2} and the value deduced from the right side of eq 6, using the data of biaxial extension, was 1.116 MN m^{-2}. We consider this agreement between these two values proof of the reliability of the data obtained from our biaxial experiment in such a small-deformation region, where the values of $\partial W/\partial I_i$ are very sensitive to both I_1 and I_2 and an especially accurate experiment is required to obtain reliable values of $\partial W/\partial I_i$. On the other hand, it is estimated that $\partial W/\partial I_2$ may take on negative values in such a small-deformation region. In the large-deformation region, the value of $\partial W/\partial I_1$ is insensitive to I_1 and decreases slightly with increasing I_2. $\partial W/\partial I_2$ is obviously a decreasing function with increasing I_2. In general, both $\partial W/\partial I_1$ and $\partial W/\partial I_2$ are dependent on I_2 rather than I_1. Similar functional forms have been observed for other vulcanizates in our previous experiments.[26,28,30,31]

On the basis of data at different temperatures shown in Figures 8 and 9, it is estimated that the form of the W function in the range of data studied is such that W may

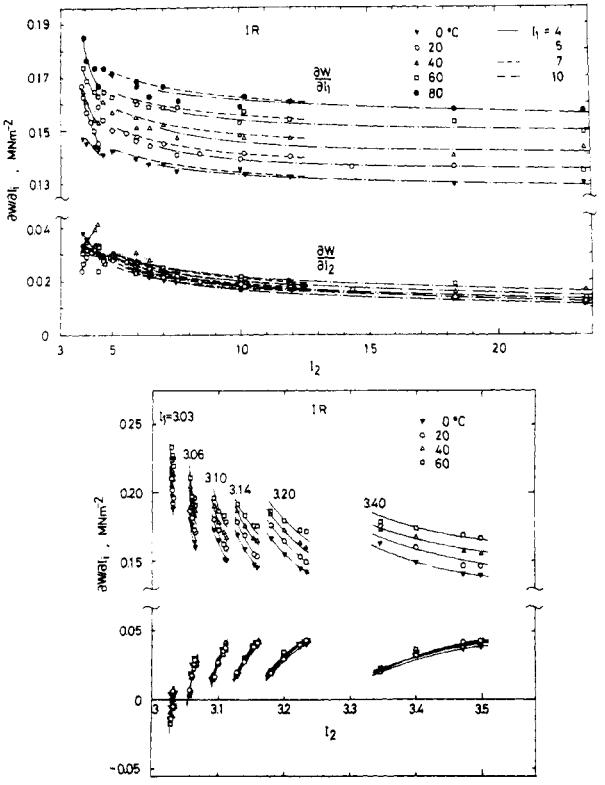

Figure 8. Temperature dependence of $\partial W/\partial I_1$ and $\partial W/\partial I_2$. The bottom part of the figure shows detail in the small-deformation region.

be given as a sum of two terms; the first term is proportional to temperature (K) and the second term is independent of temperature. That is

$$W = \alpha(I_1,I_2)T + \beta(I_1,I_2) \tag{7}$$

where α and β are functions of I_1 and I_2. Thus, the derivatives become

$$\frac{\partial W}{\partial I_1} = \frac{\partial \alpha(I_1,I_2)}{\partial I_1}T + \frac{\partial \beta(I_1,I_2)}{\partial I_1} \tag{8}$$

$$\frac{\partial W}{\partial I_2} = \frac{\partial \alpha(I_1,I_2)}{\partial I_2}T + \frac{\partial \beta(I_1,I_2)}{\partial I_2} \tag{9}$$

The value of $\partial\alpha/\partial I_1$ may be obtained from the slope of the $\partial W/\partial I_1$ vs. T relation shown in Figure 9. As already mentioned, the value of $\partial\alpha/\partial I_1$ is constant over the various deformations studied, as shown in the top portion of Figure 11 and in detail in the small-deformation region in the bottom part of this figure. One may conclude from this result that the following relation holds:

$$\partial\alpha(I_1,I_2)/\partial I_1 = C \quad (=\text{const}) \tag{10}$$

From the result that $\partial W/\partial I_2$ is independent of temperature, the following relation is deduced:

$$\partial\alpha(I_1,I_2)/\partial I_2 = 0 \tag{11}$$

Therefore, the function $\alpha(I_1,I_2)$ must be

$$\alpha(I_1,I_2) = C(I_1 - 3) \tag{12}$$

Hence, the following form of the W function is obtained from eq 7 and 12:

$$W = C(I_1 - 3)T + \beta(I_1,I_2) \tag{13}$$

The derivative forms are, therefore

$$\partial W/\partial I_1 = CT + \partial\beta(I_1,I_2)/\partial I_1 \tag{14}$$

$$\partial W/\partial I_2 = \partial\beta(I_1,I_2)/\partial I_2 \tag{15}$$

The functional form of $\partial\beta/\partial I_1$ is shown in Figure 12 with

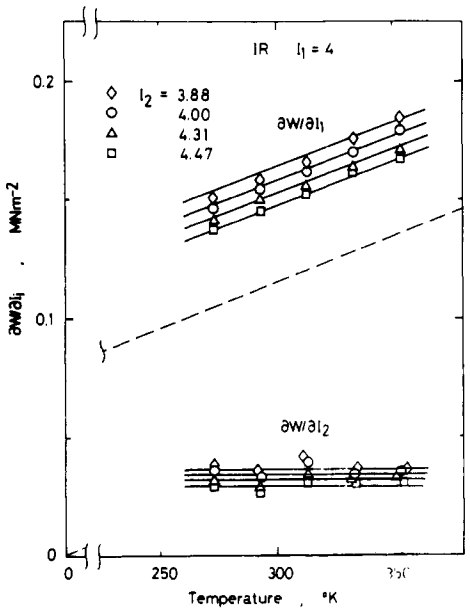

Figure 9. Temperature dependence of $\partial W/\partial I_1$ and $\partial W/\partial I_2$ for four deformations. The broken line is drawn from the point at 0 K on the abscissa so as to be parallel to the lines of $\partial W/\partial I_1$.

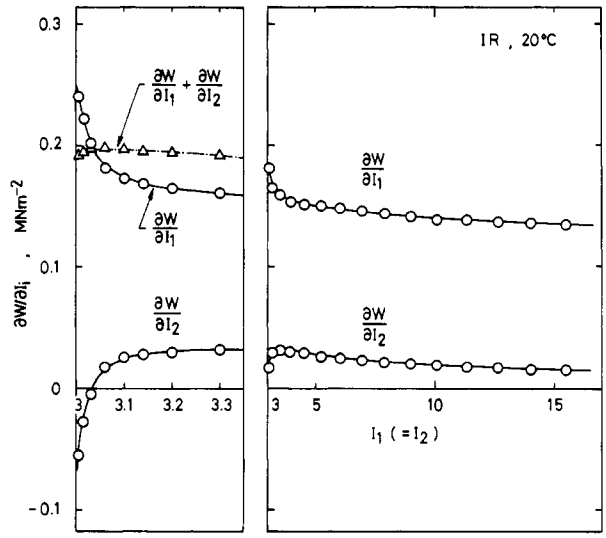

Figure 10. $\partial W/\partial I_1$ and $\partial W/\partial I_2$ for pure shear in the small-deformation region.

I_2 as abscissa. $\partial\beta/\partial I_2$ is the same as $\partial W/\partial I_2$ and its functional form has already been shown in Figure 6 and Figure 7. It is clearly shown in Figures 6, 7, and 12 that both the $\partial\beta/\partial I_1$ and the $\partial\beta/\partial I_2$ functions are independent of temperature, and the validity of eq 7 is confirmed. The first term on the right-hand side of eq 13 agrees with the form derived by kinetic theory. The second term is the other energy contribution to the W function. The separation of an energy term from the entropy term has been studied from the data of uniaxial extension by several researchers.[32-39] In our biaxial extension experiments, a separate form of the W function has resulted for a wide range of biaxial deformation. The ratio of the $\beta(I_1,I_2)$ term and the $W(I_1,I_2)$ function may be determined in our case. For example, in the case of $I_1 = 10$ and $I_2 = 10$ at 293 K, $\beta(I_1,I_2)$ accounts for 32.5% of the total value of W and this percentage is a function of I_1 and I_2 in general. Extensive research on the analysis of this ratio and comparison with the results obtained with our biaxial experiment and other researchers' results obtained with uniaxial experiments will be reported in our following papers.

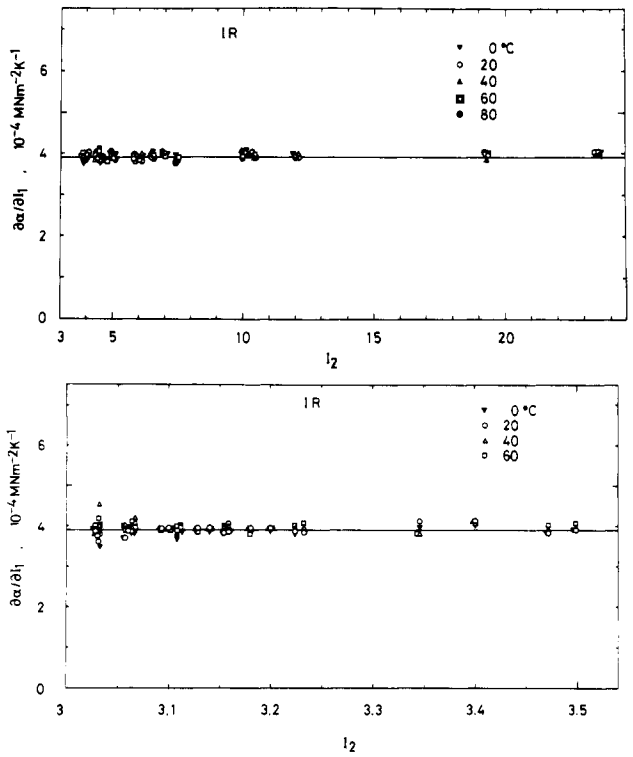

Figure 11. Deformation dependence of $\partial\alpha/\partial I_1$ for several temperature circumstances.

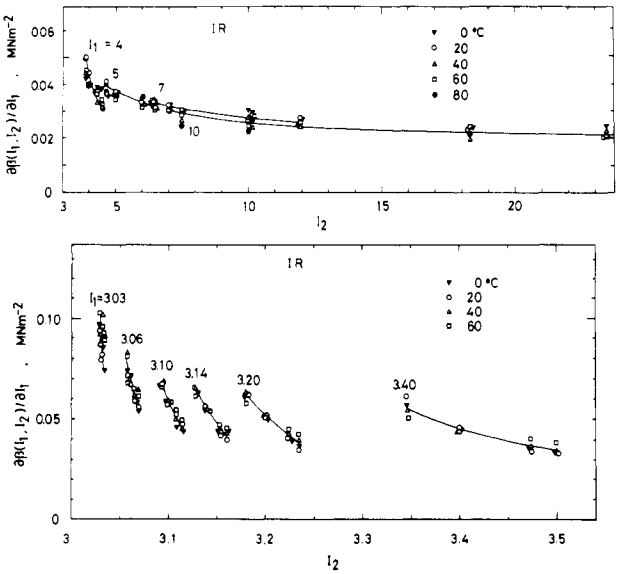

Figure 12. Deformation dependence of $\partial\beta/\partial I_1$ for several temperature circumstances.

Conclusion

In order to explain the strain energy density function of an IR vulcanizate, we have carried out experimental research with two biaxial extension devices in the temperature range 273–353 K. One of the two devices has been designed recently for the purpose of carrying out biaxial experiments in the relatively small deformation region, in which highly accurate measurements for both stress and strain are required to obtain reliable values of the derivatives of the strain energy density function.

The stress–strain measurements were carried out over the deformation ranges $3.005 < I_1 < 20$ and $3.005 < I_2 < 90$, and data from the two types of equipment smoothly overlapped each other. The isochronal values of $\partial W/\partial I_1$

Table II
Data from the Biaxial Extension Experiment at 293 K for the Isoprene Rubber Vulcanizate

λ_1	λ_2	I_1	I_2	σ_1, MN m^{-2}	σ_2, MN m^{-2}	$\partial W/\partial I_1$, MN m^{-2}	$\partial W/\partial I_2$, MN m^{-2}
1.040	0.981	3.0047	3.0046	0.0434	0	0.2102	−0.0230
	0.992	3.0052	3.0051	0.0525	0.0169	0.2379	−0.0465
	1.000	3.0062	3.0062	0.0583	0.0284	0.2510	−0.0579
	1.012	3.0085	3.0087	0.0676	0.0464	0.2570	−0.0589
	1.020	3.0107	3.0110	0.0737	0.0573	0.3485	−0.1441
	1.040	3.0180	3.0190	0.0846	0.0846	0.2705	−0.0709
1.060	0.971	3.0104	3.0100	0.0610	0	0.2060	−0.0161
	0.988	3.0115	3.0112	0.0777	0.0248	0.2224	−0.0286
	1.000	3.0136	3.0136	0.0862	0.0421	0.2290	−0.0333
	1.018	3.0187	3.0194	0.0992	0.0687	0.2167	−0.0175
	1.030	3.0234	3.0246	0.1077	0.0852	0.2502	−0.0468
	1.060	3.0393	3.0425	0.1216	0.1216	0.2246	−0.0269
1.080	0.962	3.0183	3.0173	0.0859	0	0.2025	−0.0102
	0.984	3.0201	3.0195	0.1016	0.0323	0.2109	−0.0161
	1.000	3.0237	3.0237	0.1130	0.0559	0.2074	−0.0099
	1.024	3.0326	3.0341	0.1289	0.0908	0.1829	−0.0159
	1.040	3.0407	3.0435	0.1396	0.1116	0.2112	−0.0088
	1.080	3.0678	3.0752	0.1645	0.1645	0.2058	0.0002
1.100	0.953	3.0282	3.0264	0.1064	0	0.1999	−0.0059
	0.980	3.0309	3.0298	0.1246	0.0394	0.2066	−0.0110
	1.000	3.0364	3.0364	0.1379	0.0688	0.1955	0.0023
	1.030	3.0499	3.0527	0.1565	0.1114	0.1724	0.0258
	1.050	3.0621	3.0675	0.1682	0.1368	0.1740	0.0245
	1.100	3.1030	3.1170	0.1981	0.1981	0.1852	0.0296
1.120	0.945	3.0401	3.0372	0.1257	0	0.1969	−0.0024
	0.976	3.0439	3.0419	0.1461	0.0463	0.1987	−0.0030
	1.000	3.0516	3.0516	0.1613	0.0813	0.1859	0.0117
	1.036	3.0704	3.0752	0.1827	0.1311	0.1670	0.0307
	1.060	3.0875	3.0966	0.1957	0.1608	0.1607	0.0360
	1.120	3.1443	3.1679	0.2293	0.2293	0.1704	0.0296
1.140	0.937	3.0540	3.0495	0.1434	0	0.1933	0.0003
	0.972	3.0588	3.0558	0.1669	0.0529	0.1928	0.0035
	1.000	3.0691	3.0691	0.1836	0.0936	0.1786	0.0188
	1.042	3.0941	3.1015	0.2074	0.1499	0.1638	0.0334
	1.070	3.1166	3.1308	0.2217	0.1826	0.1627	0.0338
	1.140	3.1913	3.2279	0.2570	0.2570	0.1581	0.0376
1.160	0.928	3.0697	3.0632	0.1617	0	0.1915	0.0028
	0.968	3.0757	3.0712	0.1860	0.0595	0.1842	0.0118
	1.000	3.0888	3.0888	0.2052	0.1055	0.1747	0.0228
	1.048	3.1205	3.1315	0.2306	0.1682	0.1597	0.0367
	1.080	3.1491	3.1700	0.2457	0.2051	0.1482	0.0455
	1.160	3.2435	3.2970	0.2835	0.2835	0.1493	0.0431
1.200	0.913	3.1067	3.0944	0.1960	0	0.1887	0.0063
	0.960	3.1151	3.1066	0.2233	0.0718	0.1776	0.0192
	1.000	3.1344	3.1344	0.2450	0.1283	0.1682	0.0290
	1.060	3.1817	3.2024	0.2731	0.2032	0.1510	0.0430
	1.100	3.2239	3.2633	0.2911	0.2448	0.1489	0.0436
	1.200	3.3623	3.4625	0.3297	0.3297	0.1334	0.0508
1.240	0.898	3.1505	3.1304	0.2272	0	0.1854	0.0090
	0.952	3.1615	3.1473	0.2587	0.0831	0.1753	0.0223
	1.000	3.1880	3.1880	0.2816	0.1499	0.1639	0.0329
	1.072	3.2527	3.2857	0.3121	0.2340	0.1521	0.0410
	1.120	3.3105	3.3763	0.3304	0.2820	0.1405	0.0482
	1.240	3.4982	3.6649	0.3716	0.3716	0.1243	0.0536
1.300	0.877	3.228	3.192	0.270	0	0.2126	−0.0329
	0.955	3.251	3.229	0.317	0.112	0.1917	0.0065
	0.970	3.260	3.245	0.324	0.128	0.1977	0.0012
	1.000	3.282	3.282	0.334	0.179	0.1661	0.0317
	1.045	3.324	3.353	0.341	0.224	0.1564	0.0335
	1.090	3.376	3.441	0.362	0.274	0.1510	0.0389
	1.180	3.507	3.663	0.393	0.351	0.1455	0.0405
	1.300	3.730	4.040	0.421	0.421	0.1483	0.0332
1.600	0.791	3.810	3.591	0.433	0	0.1707	0.0134
	0.910	3.860	3.718	0.489	0.177	0.1687	0.0226
	0.940	3.886	3.784	0.499	0.217	0.1662	0.0251
	1.000	3.951	3.951	0.512	0.281	0.1616	0.0270
	1.090	4.077	4.274	0.532	0.367	0.1547	0.0304
	1.180	4.233	4.673	0.544	0.424	0.1500	0.0294
	1.360	4.621	5.666	0.572	0.518	0.1423	0.0285
	1.600	5.273	7.335	0.610	0.610	0.1116	0.0257

Table II (*Continued*)

λ_1	λ_2	I_1	I_2	σ_1, MN m^{-2}	σ_2, MN m^{-2}	$\partial W/\partial I_1$, MN m^{-2}	$\partial W/\partial I_2$, MN m^{-2}
1.900	0.725	4.663	4.077	0.553	0	0.1593	0.0210
	0.865	4.728	4.315	0.607	0.218	0.1593	0.0248
	0.910	4.773	4.474	0.617	0.272	0.1576	0.0259
	1.000	4.887	4.887	0.628	0.362	0.1518	0.0272
	1.135	5.113	5.704	0.654	0.462	0.1490	0.0264
	1.270	5.395	6.720	0.664	0.522	0.1460	0.0233
	1.540	6.098	9.260	0.701	0.637	0.1389	0.0218
	1.900	7.297	13.586	0.744	0.744	0.1271	0.0202
2.200	0.674	5.749	4.607	0.651	0	0.1518	0.0251
	0.820	5.820	4.948	0.699	0.239	0.1536	0.0237
	0.880	5.881	5.246	0.711	0.315	0.1515	0.0250
	1.000	6.047	6.047	0.724	0.422	0.1474	0.0245
	1.180	6.381	7.664	0.749	0.531	0.1447	0.0221
	1.360	6.801	9.699	0.761	0.600	0.1416	0.0192
	1.720	7.868	14.863	0.809	0.735	0.1355	0.0172
	2.200	9.723	23.839	0.862	0.862	0.1233	0.0154
2.500	0.632	7.050	5.160	0.740	0	0.1475	0.0265
	0.775	7.117	5.579	0.783	0.255	0.1495	0.0233
	0.850	7.194	6.060	0.786	0.342	0.1463	0.0230
	1.000	7.410	7.410	0.809	0.473	0.1442	0.0221
	1.225	7.857	10.205	0.830	0.588	0.1406	0.0188
	1.450	8.429	13.776	0.853	0.671	0.1384	0.0163
	1.900	9.904	23.000	0.902	0.816	0.1325	0.0136
	2.500	12.383	39.383	0.974	0.974	0.1195	0.0122
2.800	0.598	8.554	5.728	0.827	0	0.1453	0.0264
	0.820	8.762	6.886	0.858	0.368	0.1426	0.0217
	1.000	8.968	8.968	0.887	0.516	0.1412	0.0197
	1.270	9.532	13.393	0.910	0.638	0.1384	0.0161
	1.540	10.265	19.143	0.942	0.735	0.1369	0.0137
	2.080	12.196	34.278	0.991	0.892	0.1305	0.0109
	2.800	15.696	61.721	1.082	1.082	0.1167	0.0098
3.100	0.568	10.255	6.304	0.919	0	0.1454	0.0247
	0.790	10.401	7.704	0.936	0.387	0.1410	0.0201
	1.000	10.714	10.714	0.959	0.557	0.1386	0.0179
	1.315	11.399	17.300	0.986	0.689	0.1355	0.0141
	1.630	12.306	26.013	1.019	0.796	0.1335	0.0119
	2.260	14.738	49.384	1.079	0.965	0.1290	0.0089
	3.100	19.231	92.560	1.190	1.190	0.1155	0.0079
3.400	0.542	12.148	6.887	1.016	0	0.1468	0.0223
	0.760	12.287	8.495	1.014	0.410	0.1399	0.0194
	1.000	12.647	12.647	1.031	0.593	0.1365	0.0163
	1.360	13.456	22.009	1.063	0.739	0.1339	0.0125
	1.720	14.548	34.624	1.088	0.853	0.1295	0.0105
	2.440	17.528	69.078	1.161	1.038	0.1262	0.0075
3.700	0.520	14.231	7.473	1.117	0	0.1490	0.0188
	1.000	14.763	14.763	1.102	0.628	0.1348	0.0149
	1.405	15.701	27.604	1.136	0.789	0.1316	0.0113

and $\partial W/\partial I_2$ at 5 min were obtained over this range by conducting biaxial stress relaxation measurements.

On the basis of the results on the temperature dependence of $\partial W/\partial I_1$ and $\partial W/\partial I_2$, we conclude that the following equations describe the functional forms of these quantities:

$$\partial W/\partial I_1 = CT + \partial\beta(I_1,I_2)/\partial I_1$$

$$\partial W/\partial I_2 = \partial\beta(I_1,I_2)/\partial I_2$$

Therefore, the form of the strain energy density function should be

$$W = CT(I_1 - 3) + \beta(I_1,I_2)$$

where C is a constant, T is temperature (K), and $\beta(I_1,I_2)$ is a function of I_1 and I_2 and independent of temperature. We have not yet obtained a simple expression of the functional form of the $\beta(I_1,I_2)$ function but only the numerical values of $\partial\beta/\partial I_1$ and $\partial\beta/\partial I_2$ under the biaxial deformation. However, it has been observed in the relatively large deformation region $I_2 > 10$ that both $\partial\beta/\partial I_1$ and $\partial\beta/\partial I_2$ (that is, $\partial W/\partial I_2$) are more sensitive to I_2 than I_1 and especially that $\partial\beta/\partial I_2$ is almost a function of I_2 only. In the small-deformation region, both $\partial\beta/\partial I_1$ and $\partial\beta/\partial I_2$ are complicated functions of I_1 and I_2. The first term on the right side of eq 13 agrees with the form of the W function based on entropy elasticity derived by the classical kinetic theory, and the second term of the equation should be a contribution of some quite different energy of the polymer network and it remains as an unsolved elasticity term from the viewpoint of molecular theory.

Acknowledgment. We thank Drs. R. F. Landel and S. T. J. Peng of the Jet Propulsion Laboratory, California Institute of Technology, for helpful advice given during the preparation of the manuscript.

References and Notes

(1) Meyer, K. H.; von Susich, G.; Valko, E. *Kolloid-Z.* **1932**, *59*, 208.

(2) Guth, E.; Mark, H. *Monatsh. Chem.* **1934**, *65*, 93.
(3) Kuhn, W. *Kolloid-Z.* **1934**, *68*, 2.
(4) Kuhn, W. *Kolloid-Z.* **1936**, *76*, 258.
(5) James, H. M.; Guth, E. *J. Chem. Phys.* **1943**, *11*, 455.
(6) Treloar, L. R. G. *Trans. Faraday Soc.* **1943**, *39*, 36.
(7) Flory, P. J.; Rehner, J., Jr. *J. Chem. Phys.* **1943**, *11*, 512.
(8) Green, A. E.; Zerna, W. "Theoretical Elasticity"; Oxford University Press: London, 1954.
(9) Eringen, A. C.; "Nonlinear Theory of Continuous Media"; McGraw-Hill: New York, 1962.
(10) Rivlin, R. S. *J. Appl. Phys.* **1947**, *18*, 444, 837.
(11) Rivlin, R. S. *Philos. Trans. R. Soc. London, Ser. A* **1948**, *241*, 379.
(12) Rivlin, R. S. *Philos. Trans. R. Soc. London, Ser. A* **1949**, *242*, 173.
(13) Rivlin, R. S. *Proc. R. Soc. London, Ser. A* **1949**, *195*, 463.
(14) Rivlin, R. S.; Saunders, D. W. *Philos. Trans. R. Soc. London, Ser. A* **1951**, *243*, 251.
(15) Rivlin, R. S.; Thomas, A. G. *Philos. Trans. R. Soc. London, Ser. A* **1951**, *243*, 289.
(16) Thomas, A. G. *Trans. Faraday Soc.* **1955**, *51*, 569.
(17) Gent, A. N.; Thomas, A. G. *J. Polym. Sci.* **1958**, *28*, 625.
(18) Rivlin, R. S.; Saunders, D. W. *Trans. Faraday Soc.* **1952**, *48*, 200.
(19) Zapas, L. J.; Craft, T. *J. Res. Natl. Bur. Stand., Sect. A* **1965**, *69* (6), 541.
(20) Mooney, M. *J. Appl. Phys.* **1940**, *11*, 582.
(21) Blatz, P. J.; Ko, W. L. *Trans. Rheol. Soc.* **1962**, *6*, 223.
(22) Miguel, A. S.; Landel, R. F. *Trans. Soc. Rheol.* **1966**, *10*, 369.
(23) Becker, G. W. *J. Polym. Sci., Part C* **1967**, *16*, 2893.
(24) Sakaguchi, K.; Kawabata, S.; Kawai, H.; Hazama, N. *J. Soc. Mater. Sci. Jpn.* **1968**, *17*, 356.
(25) Jones, D. F.; Treloar, L. R. G. *J. Phys. D: Appl. Phys.* **1975**, *8*, 1285.
(26) Kawabata, S. *J. Macromol. Sci., Phys.* **1973**, *B8* (3-4), 605.
(27) Kawabata, S.; Kawai, H. *Adv. Polym. Sci.* **1977**, *24*, 89.
(28) Kawabata, S.; Akagi, T. *Proc. 16th Jpn. Cong. Mater. Sci. 1973* **1973**, 253.
(29) Kawabata, S. *Proc. 1974 Symp. Mech. Behav. Mater.* **1974**, *2*, 299.
(30) Yoshihara, N.; Kawabata, S.; Kawai, H. *J. Soc. Mater. Sci. Jpn.* **1970**, *19*, 317.
(31) Obata, Y.; Kawabata, S.; Kawai, H. *J. Polym. Sci., Part A-2* **1970**, *8*, 903.
(32) Flory, P. J.; Hoeve, C. A. J.; Ciferri, A. *J. Polym. Sci.* **1959**, *34*, 337.
(33) Ciferri, A.; Hoeve, C. A. J.; Flory, P. J. *J. Am. Chem. Soc.* **1961**, *83*, 1015.
(34) Tovolsky, A. V.; Carlson, D. W.; Indicator, N. *J. Polym. Sci.* **1961**, *54*, 175.
(35) Roe, R. J.; Krigbaum, W. R. *J. Polym. Sci.* **1962**, *61*, 167.
(36) Natta, G.; Crepsi, G.; Flisi, U. *J. Polym. Sci., Part A* **1963**, *1*, 3569.
(37) Mark, J. E.; Flory, P. J. *J. Am. Chem. Soc.* **1964**, *86*, 1015.
(38) Shen, M.; Blatz, P. J. *J. Appl. Phys.* **1968**, *39*, 4937.
(39) Shen, M. *Macromolecules* **1969**, *2*, 358.

Calculated Intermolecular Energies Relevant to the Unusually High Melting Point of Poly(ethylene sulfide)

D. Bhaumik and J. E. Mark*

Department of Chemistry and Polymer Research Center, The University of Cincinnati, Cincinnati, Ohio 45221. *Received July 2, 1980*

ABSTRACT: Semiempirical potential energy functions were used to characterize interchain interactions in poly(ethylene sulfide) (PES) [CH_2CH_2S] and in poly(ethylene oxide) (PEO) [CH_2CH_2O], the primary purpose being to elucidate the very high melting point of PES (216 °C) relative to that of PEO (68 °C). In the case of the PEO chain, the partial charges on the atoms could be calculated by the CNDO/2 method. The charges thus obtained showed only a slight dependence on conformation, thus supporting the assumption of conformation-independent charges usually made in conformational analyses. They were also in good agreement with charges previously estimated from bond dipole moments. The total interchain interactions, significantly attractive in both polymers, were much larger in PES than in PEO, which is consistent with the interpretation of its unusually high melting point in terms of its enthalpy of fusion. The difference in intermolecular attractions is primarily due to van der Waals interactions, rather than to Coulombic (dipolar) effects. They are traceable to the fact that the S atom has twice as many electrons as the O atom, and thus a much higher polarizability. The stronger van der Waals attractions in PES are partly due to differences in crystalline state conformations, in that the S atoms in the PES (2/0) glide-plane conformation are much more exposed than the O atoms in the PEO (7/2) helix. Very approximate estimates of the crystalline state densities of the two polymers were found to be in satisfactory agreement with experiment.

The melting point T_m of any substance, including partially crystalline high molecular weight polymers, is given by the simple ratio $\Delta H_m/\Delta S_m$ of the enthalpy of fusion to the entropy of fusion.[1,2] Polymers, as might be expected, exhibit a wide range of melting points,[1-4] with those having unusually high melting points attracting particular attention because of their possible utilization as rigid materials in high-temperature applications. It is therefore of considerable interest and importance to interpret the melting point of a polymer, thermodynamically in terms of ΔH_m and ΔS_m, and molecularly in terms of the interchain interactions and chain flexibility on which these two thermodynamic qualities depend.

The polysulfides [$(CH_2)_yS$] are an unusually interesting series of molecules in this regard. They have melting points that are generally significantly higher than those of the corresponding polyoxides [$(CH_2)_yO$];[5-7] the differences are relatively large at small values of y but diminish as y increases in approaching the limiting case of polyethylene ($y = \infty$). The maximum difference occurs at $y = 2$, with poly(ethylene sulfide) (PES) [CH_2CH_2S] having a melting point of 215.6 °C[8,9] and poly(ethylene oxide) (PEO), 67.9 °C.[9,10] Elucidation of the molecular origin of this large difference in T_m, between these two structurally very similar polymers, is the major purpose of the present theoretical investigation.

A variety of information on PES and PEO of possible relevance to this problem is given in Table I. Rows three through five give some of the results, primarily theoretical, reported in two studies[9,11] of the intramolecular charac-

0024-9297/81/2214-0162$01.00/0